On the search for Galactic supernova remnant PeVatrons with current TeV instruments

Pierre Cristofari, Stefano Gabici, Régis Terrier, Brian T. Humensky

Monthly Notices of the ROYAL ASTRONOMICAL SOCIETY

MNRAS **479,** 3415–3421 (2018) doi:10.1093/mnras/sty1589
Advance Access publication 2018 June 15

On the search for Galactic supernova remnant PeVatrons with current TeV instruments

P. Cristofari,[1]★ S. Gabici,[2] R. Terrier[2] and T. B. Humensky[3]

[1]*Department of Astronomy, Columbia University, New York, NY 10027, USA*
[2]*APC, AstroParticule et Cosmologie, Université Paris Diderot, CNRS/IN2P3, CEA/Irfu, Observatoire de Paris, Sorbonne Paris Cité, 10, rue Alice Domon et Léonie Duquet, F-75205 Paris Cedex 13, France*
[3]*Physics Department, Columbia University, New York, NY 10027, USA*

Accepted 2018 June 8. Received 2018 June 2; in original form 2018 March 22

ABSTRACTS

The supernova remnant hypothesis for the origin of Galactic cosmic rays has passed several tests, but the firm identification of a supernova remnant PeVatron, considered to be a decisive step to prove the hypothesis, is still missing. While a lot of hope has been placed in next-generation instruments operating in the multi-TeV range, it is possible that current gamma-ray instruments, operating in the TeV range, could pinpoint these objects or, most likely, identify a number of promising targets for instruments of next generation. Starting from the assumption that supernova remnants are indeed the sources of Galactic cosmic rays, and therefore must be PeVatrons for some fraction of their lifetime, we investigate the ability of current instruments to detect such objects, or to identify the most promising candidates.

Key words: cosmic rays – ISM: supernova remnants.

1 INTRODUCTION

Supernova remnants (SNRs) are by far viewed as the most probable sources of Galactic cosmic rays (CRs). The requirements for a potential candidate to be the source of Galactic CRs are imposed by CR measurements. Among the most essential constraints imposed by this hypothesis, one can mention four of them: the observed level of CRs at the Earth, the CR lifetime in the Galaxy, the remarkably broad power-law energy spectrum, and the extension of this power-law spectrum up to an energy of ∼PeV, called the *knee* (Antoni et al. 2005; Bartoli et al. 2015), where the power-law spectrum breaks. Thus, if SNRs are the sources of Galactic CRs, they have to be able to meet these four essential requirements.

The observed intensity of CRs and their estimated lifetime in the Galaxy are compatible with the SNR hypothesis, provided that a fraction ≈10 per cent of the total explosion energy of the supernova progenitor is converted into CRs (Hillas 2005). Moreover, the observed power-law spectrum of CRs can be explained by the diffusive shock acceleration mechanisms (Bell 1978; Blandford & Ostriker 1978).

The last requirement, i.e. imposing that SNRs must be able to accelerate particles up to the *knee*, can also be met provided that efficient magnetic field amplification happens at SNR shocks (Bell 2004; Drury & Downes 2012). For more references, see e.g. Gabici, Gaggero & Zandanel (2016). In this hypothesis, SNRs thus have to be *PeVatrons* for some time in their lifetime. At this stage, no detection of an SNR PeVatron has been reported, but the search for such objects is strongly motivated as it would constitute major evidence in favour of the SNR hypothesis.

The recent detection of a PeVatron located in the galactic centre by the HESS Collaboration (HESS Collaboration 2016) triggered a widespread discussion in the community (see e.g. Gaggero et al. 2017; Jouvin, Lemière & Terrier 2017). Remarkably, it demonstrates the feasibility of PeVatron searches in the TeV sky, and suggests that sources other than SNRs might also accelerate PeV CRs in the Galaxy.

The observations of several SNRs in the TeV gamma-ray range have provided evidence that efficient particle acceleration is happening at SNRs shocks. Indeed, the production of gamma-rays in this range can be explained by two types of interactions. On the one hand, accelerated protons can interact with protons of the interstellar medium (ISM), and these hadronic interactions can produce gamma-rays through pion decay. On the other hand, accelerated electrons can scatter off photons of the cosmic microwave background, or other soft photon fields from stellar emission or dust, and these leptonic interactions, referred to as Inverse Compton Scattering, can produce gamma rays. Because of these two competing mechanisms, it is in most cases difficult to draw firm conclusions regarding the mechanism involved in the production of gamma rays in the TeV range (see e.g. Drury, Aharonian & Voelk 1994).

It is, however, noteworthy that above several tens of TeV, the situation becomes clearer. Because of the Klein–Nishina suppression of the cross-section for inverse Compton scattering, the production of gamma-rays via leptonic mechanisms becomes insignificant at energies above tens of TeV. Therefore, the detection of a gamma-

★ E-mail: pc2781@columbia.edu

ray spectrum extending without any attenuation up to several tens of TeV constitutes a proof for hadronic interactions (e.g. Gabici & Aharonian 2007; HESS Collaboration 2016).

In light of this fact, we propose in this article a study of the expected characteristics (e.g. flux, spectrum, angular size, etc.) that SNR PeVatrons would exhibit when observed in the TeV and multi-TeV range by current instruments. Starting from the assumption that SNRs are the sources of Galactic CRs, and using Monte Carlo simulations, we perform a population study for these objects. This will then give the expected number of SNR PeVatrons among the sources detected in the HESS Galactic Plane Survey (HESS Collaboration 2018b). We will also discuss the role of multi-wavelength observations (especially in the X-ray band), and of present and future facilities such as HAWC (www.hawc-observatory.org) and the Cherenkov Telescope Array (CTA; www.cta-observatory.org).

It has to be stressed that the detection of an SNR PeVatron by a given telescope operating in the TeV or multi-TeV domain would not necessarily imply that the detected object is indeed recognized as a PeVatron. This is because the low photon statistics in the multi-TeV domain might prevent an accurate reconstruction of the shape of the parent CR spectrum up to PeV particle energies. Therefore, the main goal of this paper is to identify the observational properties that an SNR PeVatron would exhibit when observed by currently operating gamma-ray instruments.

In this work, we rely on the approach presented in Cristofari et al. (2013, 2017). In Section 2, we briefly describe the approach and the differences with the previously cited articles. Our results are presented in Section 3 and we summarize our work in Section 4.

2 A MONTE CARLO APPROACH

The procedure used in this work was presented in Cristofari et al. (2013, 2017). We refer the reader to these papers for a more detailed description. In this approach, we begin by simulating the age and location of supernovae in the Galaxy, assuming a typical rate $\nu_{\rm SN}$ = 3/century (see e.g. Li et al. 2011, and references therein) and a spatial distribution based on the description of Yusifov & Küçük (2004) and Lorimer (2004).

The evolution of each simulated SNR is then computed following the description provided by Chevalier (1982), Bisnovatyi–Kogan & Silich (1995), Ostriker & McKee (1995), and Ptuskin & Zirakashvili (2005). Following the approach of Ptuskin & Zirakashvili (2005), we then compute the spectrum of accelerated protons and electrons, and finally the gamma-ray luminosity from each SNR shell (Cristofari et al. 2013, 2017). The gas density at the location of the simulated SNRs is taken from Nakanishi & Sofue (2003, 2006) for atomic and molecular hydrogen, respectively. The two crucial assumptions made here are: (i) protons and electrons are accelerated at the shock with a power-law spectrum $f(p) \propto p^{-\alpha}$, with p the momentum of a given particle and (ii) a fraction $\xi_{\rm CR} \sim 0.1$ of the shock ram pressure is transferred into CRs. We computed 10^3 realizations of the Galaxy, a number sufficient to study the average properties of the PeVatron population. In the following, two types of SN progenitors are considered: thermonuclear (Type Ia) with a relative rate of appearance of 0.32 and core–collapse (all other types) with relative rate 0.68 (see e.g. Ptuskin, Zirakashvili & Seo 2010). The typical parameters assumed for these two types of progenitors are summarized in Table1. In this approach, we work under the hypothesis that SNRs are the sources of Galactic CRs and provide the estimated power of Galactic CRs up to the knee, as detailed in Cristofari et al. (2013).

Table 1. Supernova parameters adopted: progenitor type, explosion energy in units of 10^{51} erg, mass of ejecta in solar masses, wind mass-loss rate in $M_\odot\ yr^{-1}$, wind speed in units of $10\,km\,s^{-1}$, and relative explosion rate. Values from Ptuskin et al. (2010).

Type	E_{51}	$M_{\rm ej,\odot}$	$\dot{M}_{-5}$	$u_{w,6}$	Relative explosion rate
Ia	1	1.4	–	–	0.32
II	1	5	4	1	0.68

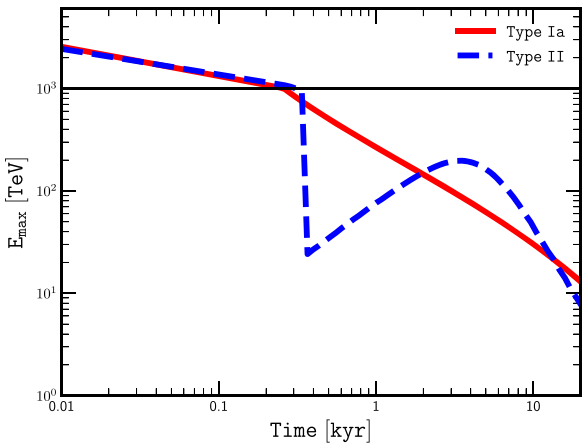

Figure 1. Maximum energy of particles accelerated at the SNR shock. The red (solid) line corresponds to Type Ia progenitors and the blue (dashed) line corresponds to Type II progenitors. In this example, the transition between the FE and SP is at ≈0.26 kyr and ≈0.3 kyr for Type Ia and Type II, respectively, where an energy of 1 PeV is reached. A density $n_0 = 1\ cm^{-3}$ is assumed for the ISM. The horizontal black line shows the 1 PeV threshold.

A central assumption done in this paper is that all SNRs are PeVatrons at some stage of their evolution and that they are the sources of the CRs observed in the region of the knee, featured at an energy $E_{\rm knee} \approx 1$ PeV. In order to reproduce the knee feature observed in the CR spectrum we have to impose that SNRs accelerate protons up to the energy $E_{\rm knee}$ at the transition between the free expansion (FE) and Sedov phase (SP) of their evolution, as illustrated in Fig. 1. In our approach, we compute $E_{\rm max} \propto u_{\rm sh}\ R_{\rm sh} B$. The discontinuity displayed for SNR from Type II progenitors at ≈0.4 kyr, and the following increasing in $E_{\rm max}$ is due to the density profile in which the shock evolves: a dense wind followed by a low-density cavity. The transition from the dense wind to the low-density region leads to a faster increase of $R_{\rm sh}$ with time that in turn results in an increase of $E_{\rm max}$. After a few kyr, the deceleration of the shock in the low-density environment leads to a decrease in $E_{\rm max}$. Such a scenario challenges current theoretical models (see e.g. Schure & Bell 2013), and is not easily testable by means of gamma-ray observations, mainly due to the poor photon statistics obtained in gamma-ray observations of SNRs in the multi-TeV band. Indeed, only a few of the SNRs observed in the TeV range have sufficient statistics to clearly test the PeVatron hypothesis, which has been disfavoured so far. This is expected since these SNRs are usually old enough to have already left their PeVatron phase, such as e.g. RXJ1713–3946 of age ≈1600 yr (HESS Collaboration 2018a). With our model we typically find a corresponding $E_{\rm max} \approx 10^2$ TeV.

For these reasons, our approach is purely phenomenological, and in the following we simply *impose* that SNRs can explain the CRs

observed at the energy of the knee: CR protons of energy $E_{\rm knee}$ escape the SNR at the transition between the FE and SPs.

The evolution of the maximum energy of accelerated particles at an SNR shock is computed assuming that particles escape once their diffusion length equals a fraction $\zeta_{\rm esc}$ of the shock radius, i.e. $E_{\rm max} \propto u_{\rm sh} B R_{\rm sh}$, where B is the magnetic field at the shock, and $u_{\rm sh}$ and $R_{\rm sh}$ the velocity and radius of the shock. Imposing 1 PeV at the transition between SP and FE amounts to making the assumption of efficient magnetic field amplification at the shock. For the ISM parameters reported in Table1 and for $E_{\rm knee} = 1$ PeV (see Fig. 1), the magnetic field upstream of the shock at the transition between FE and SP reaches $\approx 100(\zeta_{\rm esc}/0.1)^{-1}$ μG and $\approx 220(\zeta_{\rm esc}/0.1)^{-1}$ μG for Types Ia and II, respectively. These somewhat extreme values reflect the fact that it is difficult to accelerate PeV particles at SNR shocks, but they are indeed required to boost the energy of CR protons up to the PeV domain. In our approach, the value of $\zeta_{\rm esc}$ affects the value of the magnetic field amplified at the shock required to meet the condition imposed on $E_{\rm max}$ at the transition between FE and SP. Reasonable values of $\zeta_{\rm esc}$ are usually in the range 0.05−0.1, and the corresponding changes in the amplified magnetic field do not significantly affect the results presented here.

Different measurements of the position of the knee in the proton spectrum of CRs have pointed to values in the range (700 TeV–3 PeV) (Antoni et al. 2005; Bartoli et al. 2015). We will further discuss the implications that values in this range might have.

3 RESULTS AND DISCUSSION

We adopt the definition of *PeVatron* for an SNR accelerating PeV particles, i.e. $E_{\rm max} \geq 1$ PeV, and will investigate the number of PeVatron detectable by current-generation instruments, though, as stressed in Section1, their detection does not directly imply that they can be identified as PeVatron.

We start by assuming that the position of the knee is 1 PeV and by computing the number of simulated PeVatrons with an integral flux for photons of energy greater than 1 TeV above 1 per cent that of the Crab Nebula (Aharonian et al. 2006). This sensitivity is typically reached for pointed observations in ≈25 h with HESS (Aharonian et al. 2006), and here is taken as a reference value for the performances of current gamma-ray telescopes in the TeV range. In Fig. 2, the number of PeVatrons is plotted as a function of α (the assumed slope of the CR spectrum in momentum at SNR shocks) for the entire sky and for a region comparable to the one observed during the HESS Galactic plane survey: $260^\circ < l < 70^\circ$, $|b| < 3^\circ$ (HESS Collaboration 2018b). For hard spectra ($\alpha = 4.1$) the mean number of simulated PeVatrons detectable by the HESS GPS is 3.1, for 5.5 in the entire sky. For steeper spectra $\alpha = 4.4$, the number of detections is 1.7 and 0.7 for the HESS GPS and the entire sky, respectively. However, within one standard deviation (shaded regions in Fig. 2) results are compatible with no detections. In this sense, for a knee at 1 PeV (left-hand panel), our results account for the possibility of detecting a few PeVatrons, or none, depending simply on the slope of particles accelerated at the shock, and on large fluctuations between different realizations of the Galaxy. In other words, even in the optimistic scenario where we hypothesize that every SNR accelerates PeV particle at the transition between the SP and the FE, there is a reasonable situation in which no PeVatron can be detected during the HESS GPS.

Much more promising results are obtained if the value of $E_{\rm max}$ at the transition between the FE and the SP is 3 PeV (right-hand panel Fig. 2). This value is in agreement with the position of the knee reported by the KASCADE Collaboration (Antoni et al. 2005). The mean number of detections in the HESS GPS goes from $\approx 4.8^{+2.2}_{-4.8}$ to $\approx 1^{+1}_{-1}$ for α in the range [4.1–4.4]. For the entire sky, these number become $\approx 9.9^{+2.1}_{-4.9}$ and $\approx 2.3^{+0.7}_{-2.3}$, respectively.

Regardless of the value of α, the majority of the simulated PeVatrons detectable in TeV gamma-rays come from core–collapse progenitors (≥80 per cent), as illustrated by the black-dotted line of the right-hand panel of Fig. 2 (showing SNRs from Type Ia progenitors in the HESS GPS). This can be explained by two elements. First, Type II supernovae are the most abundant class (we assume here that ≈70 per cent of SNR come from Type II supernovae). Secondly, shocks from core–collapse supernovae expand in a structured medium: starting in a dense wind, they then reach a low-density cavity inflated by the wind (Weaver et al. 1977). The density of the unperturbed ISM fixes the density of the low-density bubble, therefore fixing the typical radius at which the transition from the dense wind to the low-density bubble happens. For the set of parameters assumed in this paper, SNRs from Type II progenitors that are in the PeVatron phase are all young enough to be still contained within the dense wind. The wind density is typically scaling as (Ptuskin & Zirakashvili 2005)

$$n_{\rm wind} \approx 2.2 \frac{\dot{M}_{-5}}{u_{\rm w,6}} \left(\frac{R}{\rm parsec} \right)^{-2} {\rm cm}^{-3}, \quad (1)$$

where $u_{\rm w,6}$ is the wind velocity in units of 10^6 cm s^{-1}, $\dot{M}_{-5}$ is the mass-loss rate in units of 10^{-5} M$_\odot$ yr^{-1}, and R is the radius. This wind density profiles extend up to a radius $r_{\rm w}$, where the density becomes significantly lower, of the order $\sim 10^{-2}$ cm^{-3}. $r_{\rm w}$ can be estimated by equating the wind ram pressure to the thermal pressure of the bubble interior (e.g. Cristofari et al. 2017):

$$r_{\rm w} \approx 0.9 \left(\dot{M}_{-5} u_{\rm w,6} \right)^{1/2} \left(\frac{n_0}{\rm cm^{-3}} \right)^{-19/35} {\rm pc}. \quad (2)$$

Equation (1) shows that the density profile of the wind does not depend on the location or the associated ambient ISM density, whereas for a Type Ia progenitor, the ambient density n_0 changes with the Galactic location and typically takes values in the range $\sim 0.1-1$ cm^{-3}. Because the gamma–ray luminosity is directly proportional to the density, we can therefore understand why the Type II population is dominant.

For each simulated PeVatron, we can compute the gamma-ray spectrum from pion decay and inverse Compton scattering of primary electrons accelerated at the shock, as described in Cristofari et al. (2013, 2017). In Fig. 3, the typical spectrum of an SNR PeVatron is presented for a type II supernova progenitor, $E_{\rm knee} = 3$ PeV, and for a distance of 7 kpc. We consider an electron-to-proton ratio $K_{\rm ep} = 10^{-2}$ (upper dashed curves) and $K_{\rm ep} = 10^{-5}$ (lower dashed curves). For $K_{\rm ep} = 10^{-2}$ we remark that in the TeV range the average fluxes from inverse Compton scattering and from pion decay are of the same order, while for $K_{\rm ep} = 10^{-5}$ the hadronic emission largely dominates. The uncertainty in the determination of the parameter $K_{\rm ep}$ implies that it is in general not trivial to ascribe the observed gamma-ray emission to hadronic or leptonic interactions. Remarkably, in the multi-TeV range the situation becomes unambiguous. This is because, independently on the value of $K_{\rm ep}$, the gamma-ray emission is always largely dominated by the hadronic contribution. A change in the exact value of $E_{\rm max}$ at the transition between the SP and FE phase does not significantly affect these considerations, as long as $E_{\rm max}$ remains within the PeV energy domain.

We additionally compute the spectrum of the population of secondary electrons and positrons produced from proton–proton interactions (charged pion decay), and compute the associated synchrotron emission. Secondary electrons and positrons are computed

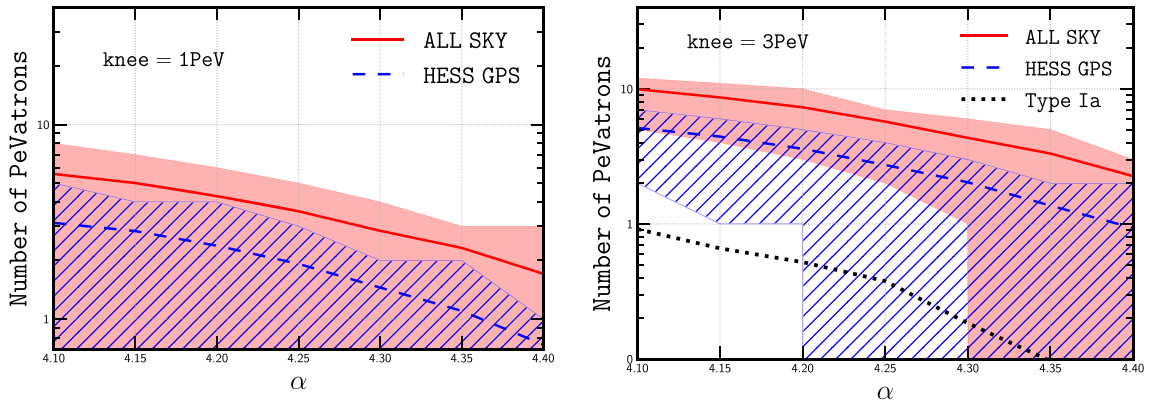

Figure 2. Number of PeVatrons with integral flux above 1 TeV greater than 1 per cent of the Crab, as a function of slope of particles accelerated at the shock α. The red (solid) line corresponds to the entire sky. The blue (dashed) line corresponds to a region $260^\circ < l < 70^\circ$, $|b| < 3^\circ$. The shaded area corresponds to ± 1 standard deviation to the mean. We assume a maximum energy reaching 1 PeV (3 PeV) at the transition between the SP and FE in the left-hand (right-hand) panel.

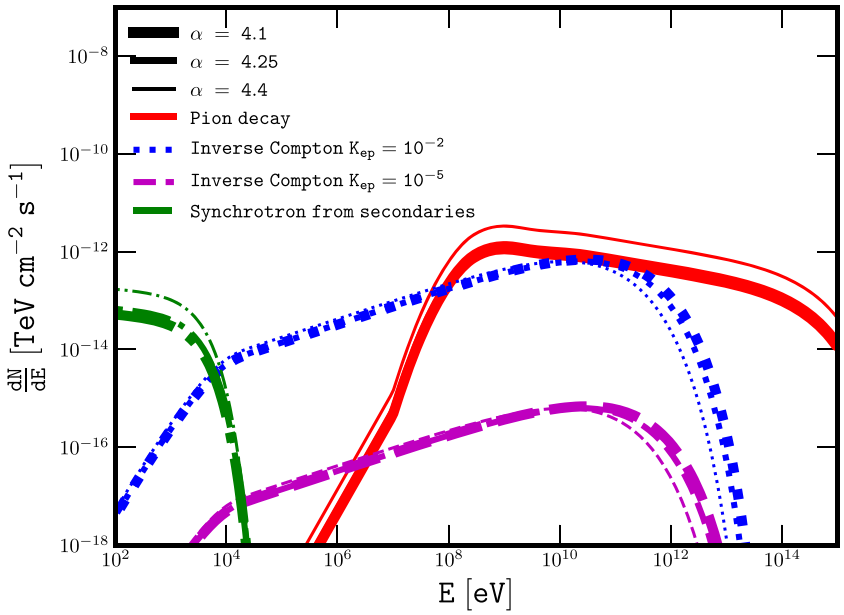

Figure 3. Differential spectra of a typical PeVatron, from Type II progenitor, of age ≈0.2 kyr and located at a distance ≈7 kpc. $E_{\rm max}$ at the transition between the SP and the FE is fixed at 3 PeV. $K_{\rm ep} = 10^{-2}$. The thick, medium, and thin lines correspond to α equal to 4.1, 4.25, and 4.4, respectively.

following the approach of Kelner, Aharonian & Bugayov (2006), and their spectrum is obtained under the assumption of fast cooling. The fast-cooling regime is only valid as long as the synchrotron loss time is shorter than the age of the SNR. We can estimate the minimum energy of electrons satisfying this condition $E_{\rm e,\,min}$ by equating the age of the considered SNR (∼0.2 kyr for the SNR represented in Fig. 3) to the synchrotron loss time,

$$\tau_{\rm sync} \approx 1.3 \left(\frac{B}{100\mu{\rm G}}\right)^{-2} \left(\frac{E}{\rm TeV}\right)^{-1} {\rm kyr}, \quad (3)$$

where E is the energy of the secondaries and B is the magnetic field. The energy of synchrotron photons emitted scales as $\propto B \times E_{\rm e}^2$, and we can estimate the minimum energy of synchrotron photons $E_{\rm sync,\,min}$:

$$E_{\rm sync,min} \approx 1.7 \left(\frac{t_{\rm age}}{\rm kyr}\right)^{-2} \left(\frac{B}{100\mu{\rm G}}\right)^{-3} {\rm eV}. \quad (4)$$

For the SNRs considered in our work, of typical age $t_{\rm age} \approx 0.1$ kyr and magnetic field ∼100 μG, $E_{\rm sync,\,min} \approx 0.17$ keV, illustrating that our approach is typically only valid in the entire X-ray domain. The synchrotron emission from secondaries corresponds to the lowest possible X-ray flux expected by an SNR PeVatron. Thus, an SNR PeVatron whose gamma-ray emission is within the reach of HESS should also unavoidably exhibit an X-ray flux roughly at the level of $\gtrsim 10^{-14}$ erg cm^{-2} s^{-1}. In fast-cooling regime, the ratio between the gamma-ray hadronic emission and the X-ray synchrotron emission from secondary electrons is a constant, and thus brighter gamma-ray SNR PeVatrons would also emit a proportionally larger X-ray synchrotron flux from secondaries.

Let us now investigate the observable properties of a typical PeVatron candidate: the integrated flux, the slope of the gamma-ray spectrum, and the angular size of the typical sources. In Fig. 4 are plotted the distributions of integral fluxes of PeVatrons for photons of energy greater than 1 TeV and 10 TeV (left-hand and right-hand panels, respectively). For these histograms, we consider a slope $\alpha = 4.25$ and $K_{\rm ep} = 10^{-2}$, and we represent the populations from Type Ia progenitors (blue filled curve), Type II progenitors (yellow hatched curve), and the sum of both (black solid line). The vertical red lines represent the typical sensitivities reached by HESS (GPS; HESS Collaboration 2018b), HAWC (5 yr; Abeysekara et al. 2017), and CTA (mCrab level, expected for the survey of the Galactic planep; Cherenkov Telescope Array Consortium et al. 2017). The distribution is centred around a median value $F\,(>1\,\mathrm{TeV}) \approx 5 \times 10^{-13}\,\mathrm{cm^{-2}\,s^{-1}}$ for the Type II progenitor and $F\,(>1\,\mathrm{TeV}) \approx 5 \times 10^{-15}\,\mathrm{cm^{-2}\,s^{-1}}$ for Type Ia, and $F\,(>1\,\mathrm{TeV}) \approx 5 \times 10^{-13}\,\mathrm{cm^{-2}\,s^{-1}}$ for the entire population. Current HESS-like TeV instruments can reach a typical sensitivity of 1 per cent of the crab, $\approx 2\text{–}3 \times 10^{-13}\,\mathrm{cm^{-2}\,s^{-1}}$ therefore roughly suggesting they could potentially detect above 1 TeV a fourth of the entire PeVatron population, mostly from core–collapse progenitors. For values of $K_{\rm ep}$ not much smaller than $\approx 10^{-2}$, the leptonic emission is expected to contribute as much as the hadronic one to the total gamma-ray emission. However, as shown in Fig. 3, the origin of the gamma-ray emission is unambiguously hadronic if we consider photon energies above $\sim$10 TeV.

For this reason, in the right-hand panel of Fig. 4 we show the distribution of integral fluxes of PeVatrons for photon energies above 10 TeV. The two types of supernovae account for two maxima centred around $F\,(>10\,\mathrm{TeV}) \approx 10^{-16}\,\mathrm{cm^{-2}\,s^{-1}}$ and $F\,(>10\,\mathrm{TeV}) \approx 10^{-14}\,\mathrm{cm^{-2}\,s^{-1}}$ for Type Ia and Type II progenitors, respectively. Typical sensitivity of HESS reaches $\approx 3 \times 10^{-14}\,\mathrm{cm^{-2}\,s^{-1}}$, suggesting, as above 1 TeV, a potential detection of a fourth of the simulated PeVatrons.

From Fig. 4, one can see that the detection potential for HAWC is better than that of HESS at 10 TeV, as expected, and that the sensitivity of CTA is large enough to probe a third of the PeVatron population.

We now comment on the spectral indices Γ of the differential gamma-ray energy spectra of the simulated PeVatrons. Fig. 5 shows the distribution of indices at 1 TeV (left-hand panel) and 10 TeV (right-hand panel) for $K_{\rm ep} = 10^{-2}$. The population from Type II progenitors and hadronic-dominated emission accounts for the harder spectra with median indices $\Gamma(1\,\mathrm{TeV}) \approx 2.3\text{–}2.4$ and $\Gamma(10\,\mathrm{TeV}) \approx 2.3$. Type Ia progenitors lead to steeper spectra with median values $\Gamma(1\,\mathrm{TeV}) \approx 2.6$ and $\Gamma(10\,\mathrm{TeV}) \approx 2.7$ and more distributed values. The PeVatrons whose gamma-ray emission is dominated by leptonic mechanisms are mostly from Type Ia progenitors with a median index $\Gamma(1\,\mathrm{TeV}) = 2.6$. At photon energies of 10 TeV the histogram is very peaked because the emission is in the large majority of cases purely hadronic and thus the slope of the gamma-ray spectrum reflects the slope of the parent proton spectrum. The plot has been produced under the assumption that all SNRs accelerate proton spectra of identical slope $\alpha = 4.25$. A dispersion in the value of α would obviously result in a broadening of the histograms.

Another important observable is the angular extension of the gamma-ray emission. For the scenario considered in this paper, the simulated PeVatrons are all quite young ($\sim$few hundred years old) SNRs. As a consequence, the radius of the SNR shell is expected to be not very large (pc scale). The median apparent angular size of the detectable PeVatrons is found to be equal to 0.8 arcmin, and over 95 per cent of sources are under 6 arcmin. In the TeV range, this corresponds to the typical point spread function of current instruments, and therefore virtually all of the potentially detectable SNR PeVatrons will be point-like, or very marginally extended.

To conclude, we comment on the cases of two young and very well-studied SNRs detected in the TeV range: Cassioppea A (Krause et al. 2008; Kumar et al. ; Ahnen et al. 2017) and Tycho (Acciari et al. 2011; Archambault et al. 2017), of age $\approx$450 yr and $\approx$350 y, respectively. Recent observations of these SNRs seem to suggest that they are not PeVatrons at the moment. In the case of Tycho, from a Type Ia progenitor this is in fact quite in agreement with our results where only $\approx$0.10 of the PeVatrons are from thermonuclear supernovae. In the case of Cassioppea A, this could be because of the very peculiar type of the progenitor (Type IIb). This rare type of progenitor, supposed to account for less than 4 per cent of all supernovae (Ptuskin et al. 2010), releases a remarkably large total explosion energy of the order of several times, 10^{51}, erg and is surrounded by an extremely dense wind, such SNR can therefore potentially enter the SP significantly sooner than other SNRs, and thus be a PeVatron for only a very short time (e.g. down to a few decades). The peculiarity of such object might explain why Cas A does not seem to fit with the general scenario described here, where such objects are not taken into account. In other words, our results can be seen as compatible with the fact that these SNRs are not active PeVatrons at the present time.

4 CONCLUSIONS

We have investigated the characteristics of the PeVatron population using simulations of the Galactic population of SNRs. As a working hypothesis, we assumed that Galactic SNRs are the sources of Galactic CRs up to PeV particle energies. In order to reproduce the observed position of the CR proton knee in the CR spectrum, the acceleration of PeV particles has to take place at the transition between the FE and SPs of the SNR evolution. We then used Monte Carlo methods to simulate the time and location of SNRs in the Galaxy, compute the evolution of the SNR shocks in the ISM using semianalytical descriptions available in the literature, and then their gamma-ray emission in the TeV and multi-TeV energy range.

In the most optimistic case, we assume $E_{\rm knee} = 3$ PeV, and that all SNRs contribute to the acceleration of particles up to the knee. The mean number of expected detections for the typical sensitivity of current instruments operating in the TeV range (we adopted here the sensitivity of HESS) is found to be in the range $\lesssim 10$ for the whole sky, the exact value depending on the value of the slope of accelerated particles assumed at the shock. The value of $\approx$10 detection is obtained for a hard spectrum of accelerated particles equal to $\alpha = 4.1$, while for spectra steeper than $\alpha = 4.3$ one could expect either few detections or no detections, depending on the exact (and a priori unknown) location of SNR PeVatrons in the Galaxy. These numbers are roughly reduced by a factor of $\approx$2 if we restrict our analysis to the region of sky covered by the GPS of HESS $260^\circ < l < 70^\circ$, $|b| < 3^\circ$. In a more pessimistic scenario where $E_{\rm knee} = 1$ PeV the expected number of detections is at most a few, and compatible within one standard deviation with no detections.

The unambiguous smoking gun of proton acceleration up to the PeV domain is the detection of an unattenuated gamma-ray emission extending up to the multi-TeV domain (e.g. Gabici & Aharonian 2007). The presence or absence of a cutoff in the multi-TeV gamma-ray spectrum can be revealed only for bright sources, such as the one recently detected in the Galactic centre region (HESS Collaboration et al. 2016). In most cases, the gamma-ray fluxes predicted in this paper for SNR PeVatrons are not bright enough to allow to identify such objects as PeV particle accelerators. However, the study

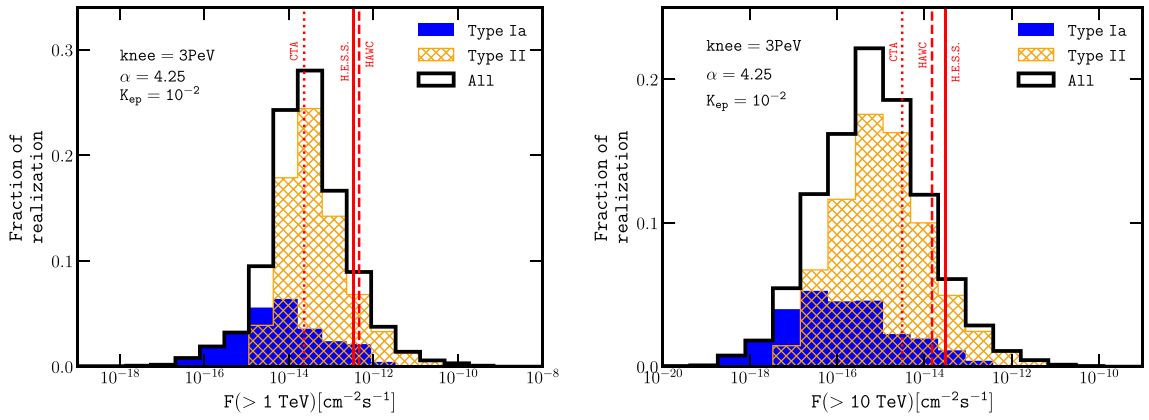

Figure 4. Integral gamma-ray flux of simulated PeVatrons for photons of energy greater than 1 TeV (left-hand panel) and 10 TeV (right-hand panel). The populations from Type Ia and Type II progenitors are represented in blue (filled) and yellow (hatched), respectively. The black (solid) curve corresponds to the sum. Vertical lines correspond to typical sensitivities of HESS (solid), HAWC (dashed), and CTA (dotted) achieved during their respective Galactic plane surveys.

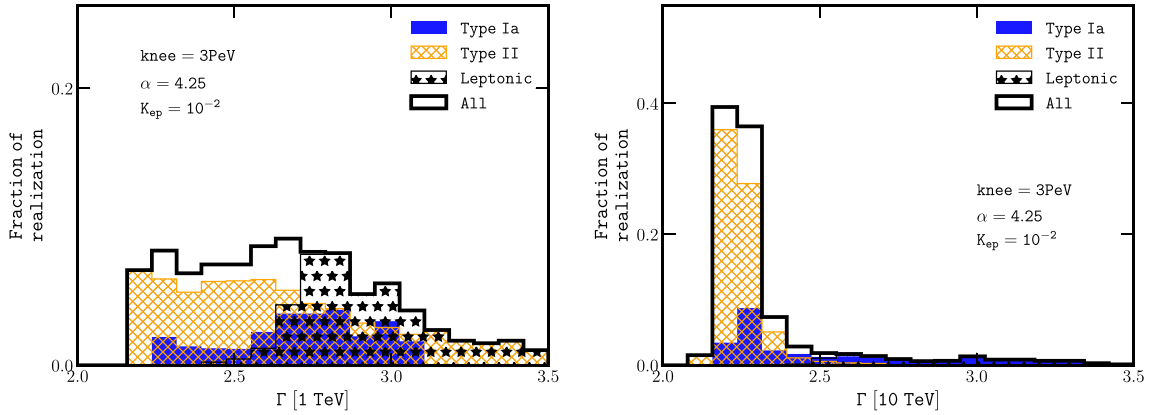

Figure 5. Gamma-ray spectral indices Γ of simulated PeVatrons for photons of energy greater than 1 TeV (left-hand panel) and 10 TeV (right-hand panel). The populations from Type Ia and Type II progenitors are represented in blue (filled) and yellow (hatched), respectively. The star-shaded area corresponds to the leptonic. The black (solid) curve corresponds to the sum. The slope in momentum of particles accelerated at the shock is $\alpha = 4.25$.

presented here demonstrates that, at least in the most optimistic scenario, current instruments might have already detected several SNR PeVatrons. Future instruments, in particular the Cherenkov Telescope Array, will increase the number of such detections and will provide us with high-quality spectra in the multi-TeV domain, which are the essential observable in order to identify CR PeVatrons. We showed in this paper that, if SNRs are the sources of Galactic CRs up to the knee, the search for PeV particle acceleration should be concentrated on to point-like or marginally extended sources showing an indication for a hard spectrum at $\gtrsim$10 TeV photon energies. As associated synchrotron X-ray flux from secondary electrons must also be present, and provides a lower limit on the observed X-ray emission from SNR PeVatrons at the level of $\gtrsim 10^{-14}$ erg cm^{-2} s^{-1} for objects whose gamma-ray flux is large enough to be detected by HESS.

In a future study, we aim at confronting the results of our simulations with the actual catalogue of known SNRs (Popkow et al. ; Acero et al. 2016; Abeysekara et al. 2017; HESS Collaboration 2018b), also considering the objects not detected in the very high-energy range, and considering the unidentified objects, in order to identify promising PeVatron candidates and orient future observations.

ACKNOWLEDGEMENTS

The authors thank D. Berge (referee) and M. Mostafá for useful comments on the draft. SG and RT acknowledge support from Agence Nationale de la Recherche (grant ANR- 17-CE31-0014) and from the Observatory of Paris (Action Fédératrice CTA). TBH acknowledges the generous support of the National Science Foundation under cooperative agreement PHY-1352567. PC acknowledges support from the Frontiers of Science fellowship at Columbia University.

REFERENCES

Abeysekara A. U. et al., 2017, ApJ, 843, 40
Acciari V. A. et al., 2011, ApJ, 730, L20
Acero F. et al., 2016, ApJS, 224, 8
Aharonian F. et al., 2006, A&A, 457, 899

Ahnen M. L. et al., 2017, MNRAS, 472, 2956
Antoni T. et al., 2005, Astropart. Phys., 24, 1
Archambault S. et al., 2017, ApJ, 836, 23
Bartoli B. et al., 2015, Phys. Rev. D, 92, 092005
Bell A. R., 1978, MNRAS, 182, 147
Bell A. R., 2004, MNRAS, 353, 550
Bisnovatyi–Kogan G. S., Silich S. A., 1995, Rev. Mod. Phys., 67, 661
Blandford R. D., Ostriker J. P., 1978, ApJ, 221, L29
Cherenkov Telescope Array Consortium, et al., 2017, preprint (arXiv:1709.07997)
Chevalier R. A., 1982, ApJ, 258, 790
Cristofari P., Gabici S., Casanova S., Terrier R., Parizot E., 2013, MNRAS, 434, 2748
Cristofari P., Gabici S., Humensky T. B., Santander M., Terrier R., Parizot E., Casanaova S., 2017, MNRAS, 471, 201
Drury L. O., Aharonian F. A., Voelk H. J., 1994, A&A, 287, 959
Drury L.O'C., Downes T.P., 2012, MNRAS, 427, 2308
Gabici S., Aharonian F.A., 2007, ApJ, 665, L131
Gabici S., Gaggero D., Zandanel F., 2016, preprint (arXiv:1610.07638)
Gaggero D., Grasso D., Marinelli A., Taoso M., Urbano A., 2017, Phys. Rev. Lett., 119, id.031101
HESS Collaboration, 2016, Nature, 531, 476
HESS Collaboration, 2018a, A&A, 612, A6
HESS Collaboration, 2018b A&A, 612, A8
Hillas A. M., 2005, J. Phys. G , 31, R95
Jouvin L., Lemière A., Terrier R., 2017, MNRAS, 467, 4622
Kelner S. R., Aharonian F. A., Bugayov V. V., 2006, Phys. Rev. D, 74, 034018
Krause O., Hattori T., Goto M., Rieke G. H., Misselt K. A., Birkmann S. M., Usuda T., 2008, Science, 320, 1195
Kumar S., for the VERITAS Collaboration, 2015, A detailled study of Gamma-ray emission from Cassiopeia A using VERITAS. in Proceedings of the 34th International Cosmic Ray Conference (ICRC 2015), The Hague, The Netherlands
Li W., Chornock R., Leaman J., Filippenko A. V., Poznanski D., Wang X., Ganeshalingam M., Mannucci F., 2011, MNRAS, 412, 1473
Lorimer D. R., 2004, in Camilo F., Gaensler B. M., eds, IAU Symp. no. 218, Astronomical Society of the Pacific , San Fransisco, USA, p. 10
Nakanishi H., Sofue Y., 2003, PASJ, 55, 191
Nakanishi H., Sofue Y., 2006, PASJ, 58, 847
Ostriker J. P., McKee C. F., 1988, Rev. Mod. Phys., 60, 1
Popkow A., 2015, The VERITAS Survey of the Cygnus Region of the Galaxy, 34, . in Proc. 34th Int. Cosm. Ray Conf. (ICRC2015), The Hague, The Netherlands, p. 750.
Ptuskin V. S., Zirakashvili V. N., 2005, A&A, 429, 755
Ptuskin V., Zirakashvili V., Seo E.-S., 2010, ApJ, 718, 31
Schure K. M., Bell A. R., 2013, MNRAS, 435, 1174
Weaver R., McCray R., Castor J., Shapiro P., Moore R., 1977, ApJ, 218, 377
Yusifov I, Küçük, I, 2004, A&A, 422, 545

This paper has been typeset from a TEX/LATEX file prepared by the author.